34th Annual International Conference of the IEEE EMBS
San Diego, California USA, 28 August - 1 September, 2012

Characterization of a novel instrument for vibration exercise

L. Xu, C. Rabotti, and M. Mischi

Abstract— **Vibration exercise (VE) has been suggested as an effective option to improve muscle strength and power performance. Several studies link the effects of vibration training to enhanced neuromuscular stimulation and typically to involuntary reflex mechanisms. However, the underlying mechanisms are still unclear and information for the most appropriate vibration training protocols is limited. This study proposes to realize a new vibration exercise system for the biceps brachii. Amplitude, frequency, and baseline of the vibrating load, which is generated by an electromechanical actuator, can be adjusted dynamically by a feedback control loop. A second-order model is employed to identify the relation between the mechanical load and the input voltage driving the actuator. An adaptive normalized least mean square algorithm is proposed to remove the motion artifacts from the measured electromyography (EMG) data. Our results show a high correlation (0.99) between the second-order model fit and the measured data, permitting accurate control on the supplied load for vibrations up to 80 Hz. Furthermore, preliminary validation with 4 volunteers showed an excellent performance in the motion artifact removal, enabling reliable evaluation of the neuromuscular activation.**

I. Introduction

Vibration exercise (VE) has been suggested as an effective methodology to improve muscle strength and power performance [1], [2], [3], mainly due to the neuromuscular demands of such vibrating loads on skeletal muscles. Various vibration devices have been realized in the last decade. Whole body vibration platforms (WBV) have been suggested to be an effective modality to exercise the lower limbs [3] while vibrating dumbbells [4], vibrating pulley-like devices [5], and vibrating barbells [6] have also been proposed for the upper limbs.

The increase in electromyography (EMG) activity observed when muscles are exposed to VE has been previously attributed to a specific reflex mechanism named tonic vibration reflex (TVR) [7]. It is well documented that TVR derives from the stimulation of the 'Ia' afferents when applying a sinusoidal stimulation directly to a muscle or a tendon [1]. However, TVR seems also to be modulated by alterations in spindle sensitivity [1], [8]. It follows that the increase in neuromuscular response observed with vibration may be the result not only of motor unit activation strategies but also of alterations in spindle sensitivity through the gamma feedback [1], [8].

Muscle tuning in response to vibrating loads seems to be affected by the characteristics of the input vibrating signal, i.e., frequency and amplitude [3], [9], as well as by muscle tension [2], [10]. As reported in previous documents, the adopted vibration frequencies were in the range of 15-60 Hz [11]. Previous studies on WBV exercise have suggested 30 Hz as the optimal training frequency for the vastus lateralis muscle [9]. However, the effect of different modulating frequencies could differ for different muscles; therefore, the optimal frequency to determine the best training stimulus might be different for different muscles.

It is evident that the underlying mechanisms leading to the measured effects of VE are still unclear and information for the most appropriate VE protocols is limited. In this study, a new isometric VE system for muscle conditioning is realized, which is portable and allows full control of the major training parameters. The load applied to the muscle is fully controlled and varied cyclically by means of a broadband actuator. Amplitude, frequency, and baseline of these cyclic variations can be dynamically and independently adjusted by a feedback control loop.

The core of the system is an electromechanical actuator, which generates a mechanical force in response to a driving input voltage. Prior to its employment, the relation between mechanical force and input voltage must be well characterized. To this end, dedicated calibration measurements were carried out making use of a load cell embedded in the system. We hypothesized that the load should be a function of the frequency and the amplitude of the driving voltage. Indeed, our preliminary tests showed that, for fixed frequency, the relation between the output force and the amplitude of the driving voltage is linear and, for fixed amplitude, the frequency response of the output force can be described by a second-order model.

The neuromuscular effects of vibration training can be studied by analyzing the EMG signal. However, previous studies have suggested that EMG measurements during VE can be severely affected by motion artifacts (MA) resulting in unwanted spectral components at the modulating frequency and its harmonics [2], [12]. MA are most probably caused by vibration-induced variations in the ionic spatial distribution in the dielectric gel of the electrodes [13]. The appearance of MA affects the EMG analysis, resulting, for example, in an overestimation of the muscle activity. In this study, an adaptive filtering approach is proposed to discriminate the neuromuscular response to vibration from MA. Based on 3D accelerometric signals recording the electrode motion, MA are estimated by an adaptive normalized least mean square (NLMS) algorithm and then subtracted from the measured EMG signal. Validation was performed on 4 volunteers.

L. Xu, C. Rabotti, and M. Mischi are with the Faculty of Electrical Engineering, University of Technology Eindhoven, 5612 AZ, Eindhoven, The Netherlands l.xu@tue.nl

II. Method

A. Prototyping

1) Actuator: The realized prototype enables performing isometric vibration exercise of the biceps brachii. Fig. 1 shows an overview of the setup. The core of the setup is a three-phase permanent magnet motor (MSK060C, Bosch Rexroth, Boxtel, The Netherlands) generating a torque consisting of a constant baseline force with superimposed vibration. The motor driver (IndraDrive HCS02, Bosch Rexroth, Boxtel, The Netherlands) is controlled by an analog function generator (PCI-5402, National Instruments, Austin, TX, USA), which is connected to a PC and controlled by dedicated software implemented in LabvView (National Instruments, Austin, TX, USA).

In order to obtain an output force which is suitable for biceps training [14], a planetary gearbox (1:10) is connected to the output shaft of the motor. Furthermore, a 50-cm aluminum bar is mounted perpendicular to the gearbox output shaft to apply a vertical force to the subject's arm.

2) Arm position and output force measurement: During vibration training, the arm position is measured using the rotary encoder embedded in the motor. This encoder generates a quadrature signal leading to a resolution of $0.28°$ at the gearbox output.

Force sensors are needed to measure the voltage-force relation of the actuator and to determine the maximum force that a subject can produce with his arm. Based on previous studies [14], the maximum force of a subject is expected to be around 300 N. Therefore, the LCAE-35kg (Omega Engineering Inc, Stamford, Connecticut, USA) load cell is chosen. This load cell uses resistance-based force sensors (strain gauges) in full bridge configuration.

A data acquisition card (PCI-6112, National Instruments, Austin, TX, USA) is used to acquire real-time data on arm position and force. In order to use the full range of the AD converter, the output signal of the load cell is amplified by an instrumentation amplifier (INA118P, Burr-Brown Corporation, Tucson, USA), which provides a high common mode rejection ratio (110 dB) and a selectable gain. The arm position can be used to provide visual feedback to the training subject while the force estimation can be used for calibration of the system as well as to estimate the maximum voluntary contraction (MVC) of the biceps.

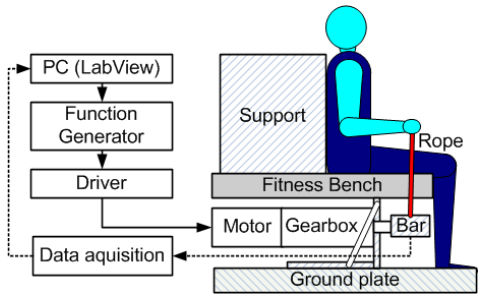

Fig. 1. Sideview of the prototype.

B. Calibration

The relation between the output force F and the input voltage V_{IN} of the actuator (Fig. 2) can be characterized by the transfer function $H(w)$, where w is the angular frequency $w = 2\pi f$. F is then measured by the embedded load cell. The load cell transforms the force F into voltage, V_{OUT}, through a function $M(F)$. Therefore, $M(F)$ has to be identified prior to the calibration. Based on the load cell specifications, $M(F)$ is constant in the frequency range of intrest and is a function of F only. To identify $M(F)$, different forces are applied to the load cell (from 0 to 300 N in steps of 10 N) and a linear regression is applied to the measured data.

The estimation of $H(w)$ is performed by applying a specific driving voltage to the motor, blocking the bar with the load cell, and measuring the output voltage of the amplifier (V_{OUT}) which can be directly translated into force by $M(F)^{-1}$.

The identification of $H(w)$ is separated into two steps: one for the DC response and one for the frequency response. For the DC response, 11 steps of DC voltage from 0 to 8.25 V are applied to the motor driver and a linear interpolation of the measurements is performed. For the frequency response, the input voltage V_{IN} is given by:

$$V_{IN}(t, w_i) = B + A \cdot sin(w_i \cdot t), \tag{1}$$

where $V_{IN}(t, w_i)$ is the time varying input voltage for given vibration frequency w_i, B the baseline DC voltage [V], and A the amplitude of the sinusoidal vibration [V]. Different B (3 V, 4 V, 5 V) are selected and a frequency range from 5 to 80 Hz is spanned with steps of 3 Hz. For each measurement, B is kept constant and the amplitude A varied from 0 to 1 V in steps of 100 mV.

Preliminary tests showed that for each constant amplitude A the data sets can be fitted by a second-order model $H(w)$, which is described by:

$$H(w_i) = \frac{k \cdot w_n^2}{-w_i^2 + 2j\xi w_n \cdot w_i + w_n^2}, \tag{2}$$

where ξ is the damping ratio, w_n is the natural frequency, and k is the gain. The data were normalized relative to the vibration amplitude A after removing the DC component given by the baseline transfer function. The model parameters ξ, w_n and k were then obtained by minimizing the mean squared error (MSE) between the measured data $\widehat{H}(w_i)$ and the absolute value of the second-order model $|H(w_i)|$:

$$\min_{\xi, w_n, k} \sum_{i=1}^{N} (\widehat{H}(w_i) - |\frac{k \cdot w_n^2}{-w_i^2 + 2j\xi w_n \cdot w_i + w_n^2}|)^2. \tag{3}$$

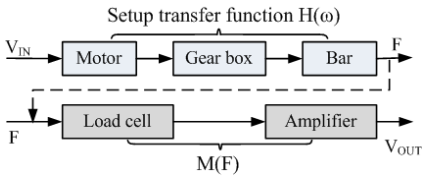

Fig. 2. Transfer function.

C. Motion artifact removal

Neuromuscular responses to VE can be estimated by EMG. The EMG amplitude increases in parallel with the intensity of muscular activity and force production [15] while the muscle fiber conduction velocity decreases in parallel with an increase in fatigue [16]. Fatigue can also be estimated by a shift in the EMG mean frequency (MF) [16].

During isometric contraction, the surface EMG was recorded from the biceps at sampling frequency $f_s = 2$ kHz. A squared grid with 64 electrodes was employed (1 mm diameter, 4 mm interelectrode distance). On top of the electrode grid, a 3D accelerometer was placed to measure the acceleration of the sensor, which is used for MA removal. An adaptive NLMS algorithm is used to estimate and remove the response of the electrical recording to acceleration.

The adaptive NLMS filter model is represented in Fig. 3. The measured EMG signal, $x[n]$, recorded at time instant n, contains the desired source $s_1[n]$ (muscle activity), which is disturbed by $m[n]$, a filtered version of the undesired source $s_2[n]$ (MA). The filter is represented by the impulse response of $s_2[n]$. The measured acceleration signal $a_b[n]$, where b is the x, y or z direction, is filtered with an adaptive FIR filter $W[n]$. The output signal $\widehat{m}[n]$, which is an estimate of $m[n]$, is then subtracted from measured EMG signal $x[n]$.

The adaptive NLMS algorithm is designed such that the square error $|e[n]|^2 = |m[n] - \widehat{m}[n]|^2$ is minimized. This is obtained by looking at the reconstructed signal $\hat{s}[n] = s_1[n] + m[n] - \widehat{m}[n]$. Minimization of $|\hat{s}[n]|^2$ implies the minimization of $|e[n]|^2$. Then, the expression of the NLMS algorithm is given as:

$$\underline{W}_{opt} = arg \min_{\underline{W}} |x[n] - \underline{a_b}[n] \cdot \underline{W}[n]|^2, \quad (4)$$

$$\underline{a_b}[n] = (a_b[n-1], a_b[n-2], \cdots, a_b[n-M]), \quad (5)$$

$$\underline{W}[n] = (W[n-1], W[n-2], \cdots, W[n-M])^t, \quad (6)$$

with $M = 60$ being the length of the adaptive filter. This is the minimum filter order beyond which the performance of the filter does not significantly improve.

The initial value of $\underline{W}$ is an empty vector $\underline{0}$. Being α the adaptive factor and σ the power of $a_b[n]$ (plus a small constant ε), the filter update is described as:

$$\underline{W}[n+1] = \underline{W}[n] + \alpha \cdot \underline{a_b}^t[n] \cdot e[n]/\sigma, \quad (7)$$

$$e[n] = x[n] - \underline{a_b}[n] \cdot \underline{W}[n], \quad (8)$$

$$\sigma = \underline{a_b}[n] \cdot \underline{a_b}^t[n]/M + \varepsilon. \quad (9)$$

This filter is applied to each of the 64 channels. Each acceleration direction $a_b[n]$ contributes to the MA and is therefore subtracted from the measured signal $x[n]$ sequentially.

Preliminary tests were carried out on four young healthy males. They performed a 20 s isometric contraction at 80% MVC with vibration at 30 Hz. Two of the enrolled volunteers performed an additional test by placing their relaxed arm on top of the arm of a subject performing isometric contraction. Also in these tests, the electrode grid and the 3D accelerometer were used. Due to the absence of contraction, these electrode signals contained MA only and could be used to validate the performance of the motion artifact removal.

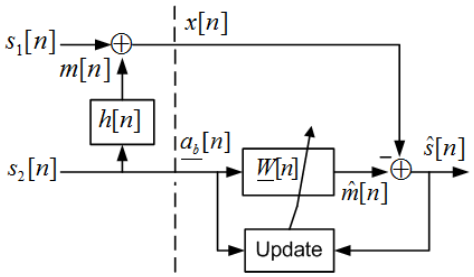

Fig. 3. Block diagram of the adaptive NLMS algorithm.

III. Results

A. Calibration

The identification of the load cell transfer function $M(F)$ revealed a linear behavior up to 300 N, with a correlation coefficient $R > 0.99$.

The DC response of the actuator was also linear ($R > 0.99$), with angular coefficient of the estimated regression line equal to 23.1 N/V.

The frequency response $H(w)$ of the full setup was also measured. Three data sets were obtained using different baselines: 3 V, 4 V, and 5 V. Fig. 4 (a) shows three fitted second-order models through the measurement data set with the baseline of 5 V, but different vibration amplitudes equal to 0.6 V, 0.8 V, and 1 V, respectively. For each of the three different baselines, an average second-order model is estimated that takes into account all the vibration amplitudes. The resulting models are shown in Fig. 4 (b). The corresponding parameters (ξ, w_n and k) and the correlation coefficients R of the fits are reported in Table I.

TABLE I
ACTUATOR PARAMETERS OF DIFFERENT CALIBRATION SETS.

set B (V)	w_n (Hz)	ξ	k	R
3	35.4	0.1889	17.91	0.9890
4	37.8	0.1801	16.50	0.9889
5	38.5	0.1577	16.82	0.9906
average	37.2	0.1756	17.05	0.9895

B. Motion artifact removal

The adaptive NLMS algorithm was applied to the recorded electrode signals and two representative examples of the results obtained in the whole data set are displayed in Fig. 5.

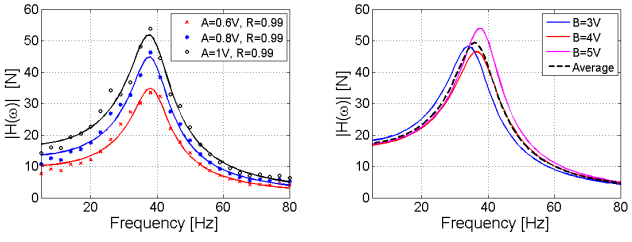

(a) (b)

Fig. 4. Second order model fits: a) Three models at baseline B=5 V; b) Averaged models.

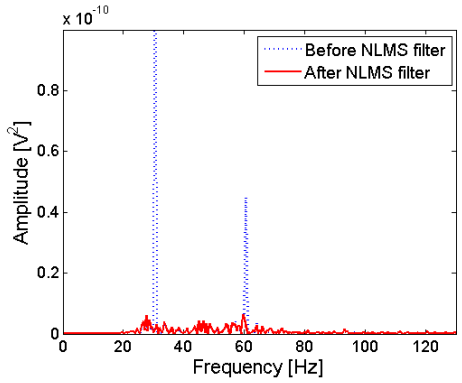

(a)

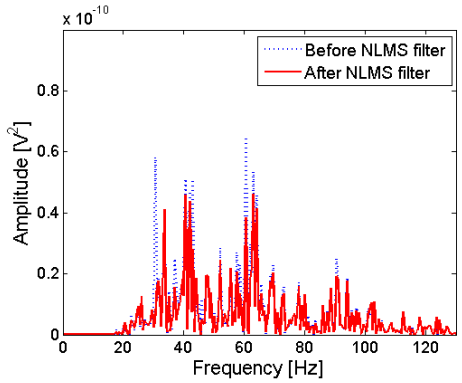

(b)

Fig. 5. Power spectrum before and after NLMS filtering for: a) a signal containing MA only and b) a signal containing both EMG and MA.

Fig. 5 (a) shows the results after applying the filter to a signal containing the interference due to MA only. It is clear that the high peak spectrum at the vibration frequency 30 Hz and its harmonics are efficiently canceled by the adaptive filter.

Fig. 5 (b) shows an example of the results on a signal containing both EMG and MA. A decrease in the 30 Hz, 60 Hz, and 90 Hz amplitude is clearly visible, while the rest of the spectrum remains comparable.

IV. Discussion and Conclusions

This study presents a new VE system for the biceps brachii. Frequencies up to 80 Hz and forces up to 300 N can be reached. This is sufficient for biceps training [14]. The calibration of the prototype shows a high correlation between a second-order model fit and the measured response of the actuator. However, the resonance frequencies of the second-order model seem to increase as the baseline increases. This effect is most probably to be ascribed to the nonlinear behavior of the elastic components in the transmission chain, including the shafts as well as the aluminum bar.

The influence of MA may result in overestimation of the EMG power or in inaccurate estimation of muscle fiber conduction velocity [2], [14], [17]. These are essential EMG features for the characterization of muscle performance. In this study, an adaptive NLMS algorithm is proposed to decorrelate the EMG signal induced by sensor motion and the real EMG signal. This NLMS algorithm produces efficient filtering of the vibration frequencies and its harmonics. Compared to other studies that force the vibration frequency components to zero [2], [18], the proposed NLMS algorithm indicates that neuromuscular response around the vibration frequency is present, and enables future studies on neuromuscular responses, such as tonic vibration reflex and muscle fiber recruitment, also at the vibration frequency [2], [18], [19].

In conclusion, the realized system provides a suitable platform to study the the combined effect of muscle tension and vibration on muscle activation. Such a system enables new studies to identify and model the physiological processes enhanced by VE, possibly bringing new insight on neuromuscular reflex and activation pathways.

References

[1] L. Bongiovanni, K. Hagbarth, and L. Stjernberg, "Prolonged muscle vibration reducing motor output in maximal voluntary contractions in man," *J Physiol*, vol. 423, pp. 15–26, 1990.

[2] M. Mischi and M. Cardinale, "The effects of a 28-hz vibration on arm muscle activity during isometric exercise," *Med Sci Sports Exerc*, vol. 41, no. 3, pp. 645–652, 2009.

[3] M. Cardinale and J. Lim, "The acute effects of two different whole body vibration frequencies on vertical jump performance," *Med Sci Sports Exerc*, vol. 56, pp. 287–292, 2003.

[4] C. Bosco, M. Cardinale, and O. Tsarpela, "Influence of vibration on mechanical power and electromyogram activity in human arm flexor muscles," *Eur J Appl Physiol*, vol. 79, no. 4, pp. 306–311, 1999.

[5] V. Issurin and G. Tenenbaum, "Acute and residual effects of vibratory stimulation on explosive strength in elite and amateur athletes," *J Sports Sci*, vol. 17, no. 3, pp. 177–182, 1999.

[6] B. Poston, W. Holcomb, and M. Guadagnoli, "The acute effects of mechanical vibration on power output in the bench press," *J Strength Cond Res*, vol. 21, no. 1, pp. 199–203, 2007.

[7] K. Hagbarth and et al., "Single unit spindle responses to muscle vibration in man," *Prog Brain Res*, vol. 44, pp. 281–289, 1976.

[8] E. Ribot-Ciscar, C.Rossi-Durand, and J. Roll, "Increase muscle spindle sensitivity to movement during reinforcement manoeuvres in relaxed human subjects," *J Physiol*, vol. 523, pp. 271–282, 2000.

[9] M. Cardinale and J. Lim, "Electromyography activity of vastus lateralis muscle during whole-body vibrations of different frequencies," *J Strength Cond Res*, vol. 17, no. 3, pp. 621–624, 2003.

[10] J. Wakeling and B. Nigg, "Modification of soft tissue vibrations in the leg by muscular activity," *J Appl Physiol*, vol. 90, no. 2, pp. 412–420, 2001.

[11] M. Cardinale and J. Rittweger, "Vibration exercise makes your muscles and bones stronger: fact or fiction?" *J Br Menopause Soc*, vol. 12, no. 1, pp. 12–18, 2006.

[12] A. Abercromby, W. Amonette, C. Layne, and et al., "Variation in neuromuscular responses during acute whole-body vibration exercise," *Med Sci Sports Exerc*, vol. 39, no. 9, pp. 1642–1650, 2007.

[13] J. G. Webster, *Medical Instrumentation Application and Design*. Wiley, 2009.

[14] M. Mischi and et al., "Electromyographic hyperactivation of skeletal muscles by time-modulated mechanical stimulation," in *29th Annual International Conference of the IEEE*, aug. 2007, pp. 5373–5376.

[15] R. Enoka, "Muscle strength and its development," *Sports Med*, vol. 6, pp. 146–168, 1988.

[16] R. Merletti and et al., "Myoelectric manifestations of fatigue in voluntary and electrically elicited contractions," *J Appl Physiol*, vol. 69, pp. 1810–1820, 1990.

[17] A. Fratini and et al., "Relevance of motion artifact in electromyography recordings during vibration treatment," *J Electromyogr Kines*, vol. 19, no. 4, pp. 710–718, 2009.

[18] B. Martin and H.-S. Park, "Analysis of the tonic vibration reflex: influence of vibration variables on motor unit synchronization and fatigue," *Eur J Appl Physiol*, vol. 75, no. 6, pp. 504–511, 1997.

[19] R. Ritzmann, A. Kramer, M. Gruber, and et al., "Emg activity during whole body vibration: motion artifacts or stretch reflexes?" *Eur J Appl Physiol*, vol. 110, no. 1, pp. 143–151, 2010.